Phys Chem Minerals (2002) 29: 10–18
DOI 10.1007/s002690100198

ORIGINAL PAPER

B. Lavina · G. Salviulo · A. Della Giusta

Cation distribution and structure modelling of spinel solid solutions

Received: 19 February 2001 / Accepted: 1 June 2001

Abstract This paper presents an improved generalisation of cation distribution determination based on an accurate fit of all crystal-chemical parameters. Cations are assigned to the tetrahedral and octahedral sites of the structure according to their scattering power and a set of bond distances optimised for spinel structure. A database of 295 spinels was prepared from the literature and unpublished data. Selected compositions include the following cations: Mg^{2+}, Al^{3+}, Si^{4+}, Ti^{4+}, V^{3+}, Cr^{3+}, Mn^{2+}, Mn^{3+}, Fe^{2+}, Fe^{3+}, Co^{2+}, Ni^{2+}, Zn^{2+} and vacancies. Bond distance optimisation reveals a definite lengthening in tetrahedral distance when large amounts of Fe^{3+} or Ni^{2+} are present in the octahedral site. This means that these cations modify the octahedral angle and hence the shared octahedral edge, causing an increase in the tetrahedral distance with respect to the size of the cations entering it. Some applications to published data are discussed, showing the capacity and limitations of the method for calculating cation distribution, and for identifying inconsistencies and inaccuracies in experimental data.

Keywords Spinel · Cation distribution · Bond distances · Structure modelling

Introduction

Determination of cation site partitioning is crucial in the characterisation of geological and technological materials. Spinels sensu latu are important minerals and industrial materials because they are used for semiconductors, magnetic and refractory materials, pigments, and natural and synthetic gems, and they are also the main ores yielding several elements. They are responsible for most magnetism in rocks, occurring as accessory minerals in igneous and metamorphic rocks. In natural spinels, cations are mainly Mg^{2+}, Al^{3+}, Ti^{4+}, V^{3+}, Cr^{3+}, Mn^{2+}, Mn^{3+}, Fe^{2+}, Fe^{3+} and Zn^{2+}. An Mg-rich silicate spinel is most probably the main component of the lower part of the upper mantle.

Details of spinel structure, fully described in Hafner 1960, Hill et al. 1979 and O'Neill and Navrotsky 1983, are summarised in Appendix 1.

Thermodynamic modelling of spinels has been undertaken by several authors. On the basis of available data, O'Neill and Navrotsky (1983, 1984) proposed quadratic dependence on x, the inversion parameter describing the cation distribution in binary spinels of the type $^{IV}(A_{1-x}B_x)\ ^{VI}(A_xB_{2-x})O_4$, for electrostatic contribution to lattice energy.

Della Giusta and Ottonello (1993), with a wider database, found that static potentials in aluminate and ferrite spinels depend on x to a greater extent, and this emphasises the importance of accurate knowledge of x, since cation distribution makes an important contribution to thermodynamic stability via changes in coulombic and repulsive energies, and configurational entropy.

In this paper, we face a basic difficulty in all good modelling, i.e. the accuracy of cation distribution determination. This is really a crucial point since, for example, considering an extensively investigated spinel like $MgAl_2O_4$, extremely scattered data are reported. In Maekawa et al. (1997) and Andreozzi et al. (2000), the inversions measured by different authors at the same temperature differ by as much as 0.15 afu (atoms per formula unit). We must recall that, in previously quoted models, such a difference corresponds to a range of about 700 °C in the calculated equilibrium temperature, preventing any use of Mg–Al-rich spinels as geospeedometers or geothermometers.

B. Lavina (✉) · G. Salviulo · A. Della Giusta
Dipartimento di Mineralogia e Petrologia,
Università di Padova, Corso Garibaldi 37,
35137, Padova, Italy
Tel.: +39-49 8272032;
Fax: +39-49-8272010
e-mail: barbara@dmp.unipd.it

Procedure and assumptions

The method discussed here is an improved generalization of that previously used by several authors, e.g. O'Neill and Navrotsky

(1983), Marshall and Dollase (1984) and Della Giusta et al. (1996). This model yields cation distribution by minimising the weighted differences between observed crystal-chemical data and data calculated from site atomic fractions. Cation distribution in the tetrahedral (T) and octahedral (M) sites must be consistent with the following assumptions:

1. The mean atomic number (m.a.n.) of the site, linear with site population, corresponds to:

$$\text{m.a.n.}_{\text{T}} = \sum_i {}^{\text{IV}}X_i N_i \quad (1)$$

$$\text{m.a.n.}_{\text{M}} = \sum_i {}^{\text{VI}}X_i N_i \ , \quad (2)$$

where ${}^{\text{IV}}X_i$ and ${}^{\text{VI}}X_i$ are chemical species in T and M respectively, and N is their atomic number. For literature data, m.a.n. values must often be recalculated from the proposed distribution, since site-scattering values are usually not supplied, in spite of the recommendation of Hawthorne et al. (1995).

2. The site bond length arises from a linear contribution of each species to the tetrahedral (T–O) and octahedral (M–O) coordination distances (O'Neill and Navrotsky 1983; Marshall and Dollase 1984; Waerenborgh et al. 1994; Della Giusta et al. 1996):

$$\text{T}-\text{O} = \sum_i {}^{\text{IV}}X_i \, {}^{\text{IV}}D_i \quad (3)$$

$$\text{M}-\text{O} = \sum_i {}^{\text{VI}}X_i \, {}^{\text{VI}}D_i \ , \quad (4)$$

where ${}^{\text{IV}}D_i$ and ${}^{\text{VI}}D_i$ are the cation-to-oxygen bond distances of each cation in tetrahedral and octahedral coordination, respectively.

Condition 1 alone yields the cation distribution in end-member spinels from diffraction data, if the electronic or nuclear scattering power of the two cations differs appreciably. When more than two cations enter one or both sites, as usually occurs in natural samples, condition II is very helpful, since a chemical species in a crystal structure is characterised not only by its atomic number but also by its bond distance in a given coordination. Shannon's 1976 radii are a powerful tool for good simulation of a large number of structures and also for cation site assignment. It is noteworthy that Shannon's cation-to-oxygen bond distances need some rearrangement if fine structural details are to be investigated within a single structure type.

To solve the problem of cation site assignment, several authors consider bond valence requirements which need minimisation of the differences, for each site, between the sums of the formal valences and the sum of the bond valence: this, too, is a very useful tool, especially for sites with uneven bond distances, as applied by Wright et al. (2000) following the formulation of Brown and Altermatt (1985) and Brese and O'Keeffe (1991). In any case, this formulation is subject to the same criticism applied to the generalised application of Shannon's bond distances. It can help in providing good initial assignment of the occupancies, but it needs to be adapted to each structural type if accurate cation distributions are required, as stressed by Wright et al. (2000). In spinels, as all the bond distances of each polyhedron are equal, it supplies the same information as rearranged bond distances. Moreover, since there is only one oxygen anion, its charge balance does not depend on the cation distribution between T and M sites.

In sum, site atomic fractions ${}^{\text{IV}}X_i$ and ${}^{\text{VI}}X_i$ must satisfy Eqs. (1)–(4). They must also total the atomic proportions from chemical analysis and obey three crystal-chemical constraints: occupancies of T and M sites and formal valence, 1, 2 and 8 respectively, referring to a general formula AB_2O_4. ${}^{\text{IV}}X_i$ and ${}^{\text{VI}}X_i$ may be calculated by minimising the following sum of residuals:

$$F(X_i) = \frac{1}{n}\sum_1^n{}_j \left(\frac{O_j - C_j(X_i)}{\sigma_j}\right)^2 \ , \quad (5)$$

where O_j are the observed quantities with their standard deviation σ_j. O_j are the four observed crystallographic parameters (a, u and m.a.n. of T and M sites) and the chemical atomic proportions (at least two) for a total of n. $C_j(X_i)$ are the corresponding quantities calculated by means of variable cation fractions X_i. $F(X_i)$ values of less than 1 mean good agreement between calculated and observed data.

It is possible to use Eq. (5) considering as variable parameters, for instance, only ${}^{\text{IV}}X_i$, as ${}^{\text{VI}}X_i$ are the differences between ${}^{\text{IV}}X_i$ and the corresponding chemical atomic proportion. ${}^{\text{IV}}X_i$ may also be decreased by one unit by applying the occupancy constraint rigorously.

We tested this procedure extensively, but the distributions turned out to depend on the chosen variable parameters. This is probably due to the uneven accuracy of the experimental data.

Consequently, our adopted strategy was to consider all ${}^{\text{IV}}X_i$ and ${}^{\text{VI}}X_i$ as variable parameters, and to include the three crystal-chemical constraints in Eq. (5) among the residuals. All the constraints were assigned $\sigma = 0.0005$, an empirical value which generally brings occupancies to within 10^{-3} of the theoretical value, an uncertainty fully consistent with the accuracy of chemical data. The number n of residuals in Eq. (5) is consequently at least nine. Minimisation was performed by SIDR, a routine written for the MINUIT system for function minimisation by James and Roos (1975).

Bond distance optimisation

Atomic fractions obtained through Eq. (5) depend on the adopted set of crystal radii; thereafter, we refer to the cation-oxygen bond distance, for each cation.

We performed a general rearrangement of bond distances by preparing a database (available from the authors on request) which includes all published data containing determinations of cell parameter, oxygen coordinate and cation distribution, with their standard deviations, plus other unpublished data. The database contains 295 samples, including defect specimens. Table 1 lists some data about the occurrences of each cation in each site, i.e. mean and maximum contents in afu and distribution in five frequency classes.

Distribution is uneven: Al, Mg, Fe^{2+}, Zn and Fe^{3+} are by far the most frequently represented cations in the database, and consequently we must expect greater accuracy in the determination of their bond distances with respect to those present in lesser amounts. Table 1 reveals the strong octahedral preference of Cr, V, Mn^{2+} and Ti in spinel structure, and that for the tetrahedral site of Si. The remaining cations, although having a general preference for definite coordinations like Zn and Mg for T or Al and Fe^{3+} for M, may assume both coordinations, in competition with other cations.

For bond distance optimisation, we prepared a computing system based on a modified version of the MINUIT code (James and Roos 1975). A main routine controlled the D_i variables of Eqs. (3), (4), and the starting values of O'Neill and Navrotsky (1983) were used, or, if missing, those of Shannon (1976), to minimise the function:

$$G(D_i) = \frac{\sum F(X_i)}{N} \ , \quad (6)$$

where $F(X_i)$ is the function defined by Eq. (5) and N is the number of samples in the database.

A first minimisation run was performed, allowing site atomic fractions to vary within twice their reported standard deviations, or within 30% for distributions

reported without σ. No limits were assigned to unpublished samples. Cations with atomic fractions lower than 0.02 afu were fixed and assigned to T or M site according to their general site preference, as evidenced by the mean values of Table 1.

For magnetite-rich compositions, it was necessary to take into account the electron-hopping effect on bond distances. This was done by assuming 2.059 Å as the bond distance for $Fe^{2.5+}$ species in M site, that is, the M–O bond distance of pure magnetite (Hamilton 1958; Fleet 1981; Wechsler et al. 1984) and assuming that octahedral iron is charge-hopping when the ratio of ferric to ferrous iron approaches 1. It was not necessary to consider different ratios within our database. However, this point will deserve further consideration – when other compositions are available – of the correct definition of the amounts of ferric and ferrous iron involved in charge-hopping, as discussed by Marshall and Dollase (1984).

This minimisation led to high $F(X_i)$ values (close to 10) for ferrites, due to large residuals Δ(T–O) – the difference between observed and calculated tetrahedral distance – up to 0.022 Å, and to an unacceptable tetrahedral bond distance for Ni. Figure 1a shows the distribution of Δ(T–O) versus the amount of ${}^{VI}X_{Fe^{3+}}$ for synthetic ferrites: observed T–O distances are systematically greater than calculated ones. This points to lengthening of the tetrahedral distance – no matter which tetrahedral cations are involved – due to the presence of Fe^{3+} in the octahedron.

In order to correct the T–O distances for these effects, considering the large scatter of data in Fig. 1a, a reasonable approach was to modify Eq. (3) as follows:

$$T-O = \sum_i {}^{IV}X_i \, {}^{IV}D_i + k_1 \, {}^{VI}X_{Fe^{3+}} \quad (7)$$

This equation, still linear, is a first empirical attempt to account for the effect of ${}^{VI}X_{Fe^{3+}}$ by fitting coefficient k_1.

Table 1 Occurrences of tetrahedral and octahedral cations in spinel database. Mean and maximum contents in afu and number of samples distributed in five frequency ranges

	Al	Fe^{2+}	Fe^{3+}	Mg	Mn^{2+}	Mn^{3+}	Si	Cr	Zn	V	Ni	Ti	Vac	Co
T site														
Mean	0.158	0.120	0.105	0.286	0.065	0	0.031	0	0.185	0	0.019	0.000	0	0.034
Max	0.873	1.000	1.000	1.000	1.001	0	1.000	0	1.000	0	1.000	0.000	0	1.000
Frequency ranges distribution														
0.02–0.2	104	50	86	34	4	0	0	0	12	0	23	0	0	0
0.2–0.4	36	40	3	16	18	0	0	0	3	0	4	0	0	0
0.4–0.6	3	11	2	24	5	0	0	0	4	0	0	0	0	0
0.6–0.8	9	7	16	60	5	0	0	0	15	0	0	0	0	5
0.8–1.0	22	10	13	24	8	0	9	0	42	0	1	0	0	7
M site														
Mean	0.988	0.091	0.323	0.128	0.019	0.002	0.000	0.209	0.014	0.057	0.093	0.053	0.004	0.017
Max	1.992	1.990	1.990	1.990	1.009	0.193	0.024	2.000	1.000	2.000	1.990	1.000	0.219	1.986
Frequency ranges distribution														
0.02–0.4	16	27	84	116	20	9	1	18	37	10	0	8	7	11
0.4–0.8	7	10	4	14	4	0	0	6	0	7	5	2	0	0
0.8–1.2	34	11	19	9	1	0	0	5	1	0	23	14	0	1
1.2–1.6	17	2	14	0	0	0	0	13	0	0	0	0	0	0
1.6–2.0	125	2	26	1	0	0	0	18	0	5	2	0	0	1

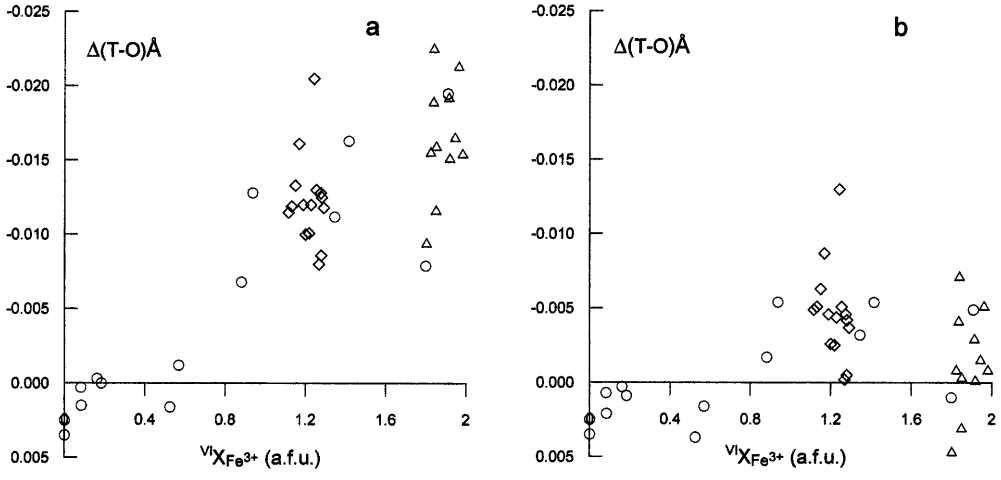

Fig. 1a, b Differences between calculated and observed T–O distances as a function of octahedral iron contents. **a** Using Eq. (4) **b** Using Eq. (7). *Triangles* O'Neill 1992; *diamonds* O'Neill et al. 1992; *circles* Waerenborgh et al. 1994

Minimisation was then repeated by calculating the bond distances through Eqs. (4) and (7). The $F(X_i)$ function of ferrites decreased from about 10 to less than 1, and the differences shown in Fig. 1a were greatly reduced (Fig. 1b), almost all the residuals being within 2σ of the experimental data of the database.

Concerning Ni, we estimated 2.054 Å for $^{VI}D_{Ni}$ and 2.045 Å for $^{IV}D_{Ni}$. This value was not acceptable either according to Shannon's systematics or to the T–O, 1.94 Å, in the normal spinel $NiCr_2O_4$ (Hill et al. 1979). Unfortunately, Ni in the database is combined almost exclusively with Al. In any case, within the reliability of the compositions applied, we provisionally explained this as a possible effect of lengthening of the tetrahedral distance due to $^{VI}X_{Ni}$, like $^{VI}X_{Fe^{3+}}$, and an analogous correction was consequently applied:

$$T-O = \sum_i {}^{IV}X_i\,{}^{IV}D_i + k_1\,{}^{VI}X_{Fe^{3+}} + k_2\,{}^{VI}X_{Ni} \qquad (8)$$

Since the available data on Ni compositions are insufficient to determine both distances and k_2, we fixed the $^{IV}D_{Ni}$ distance to the previously quoted value, whereas $^{VI}D_{Ni}$ and k_2 were allowed to vary.

Minimisation was again performed by calculating the bond distances through Eqs. (4) and (8).

Results are reported in Table 2, compared with the values of Shannon (1976) and O'Neill and Navrotsky (1983). Standard deviations, as expected, are greater for species poorly represented in the database, like $^{VI}D_{Mn^{3+}}$ and $^{VI}D_{Zn}$, but high σ values are also shown by some species with high frequency or mean value.

The case of Ni is interesting: in spite of the fact that it is involved only with Al, which has one of the lowest σ in Table 2, and that coefficient k_2 substantially acts only on Ni aluminate compositions, $^{VI}D_{Ni}$ has $\sigma = 0.01$ Å. The same happens for $^{IV}D_{Si}$ but not for $^{IV}D_{Co}$, in spite of similar frequencies and mean amounts. This suggests that the database includes some partially unreliable data, but we could not exclude them, since some atomic species would otherwise be insufficiently represented. We outline that the used database of 295 samples was obtained rejecting all the samples for which the a_{obs}–a_{cal} residual was greater than 0.02 Å.

From Table 2, the mean increase in bond distance from tetrahedral to octahedral coordination for the eight cations involved in both coordinations is 0.14 Å, with a minimum of 0.12 Å for Mg and a maximum of 0.17 Å for Zn. These values range from 0.14 to 0.17 Å in Shannon (1976) and from 0.12 to 0.16 Å in O'Neill and Navrotsky (1983). Table 2 also shows the improved self-consistency of the new set of distances with respect to the quoted authors, as shown by the $G(D_i)$ function.

As Table 3 shows, all the structural and chemical parameters in the database are satisfactorily reproduced with the optimised bond distances listed in Table 2.

With these bond distances, more accurate previsions about the behaviour of spinel structure are possible. For example, they correctly predict the cell volume increase in

Table 2 Proposed set of optimised bond distances compared with previous sets, and resulting values of function $G(D_i)$ (see text). $^{VI}D_{Si}$ is taken from stishovite (Ross et al. 1990)

$G(D_i)$	Shannon (1976) 14	O'Neill and Navrotsky (1983) 7.3	This paper 1.1	Standard deviations
Tetrahedral bond distances				
Al	1.77	1.77	1.774	0.001
Fe^{2+}	2.01	1.995	2.000	0.001
Fe^{3+}	1.87	1.865	1.875	0.002
Mg	1.95	1.965	1.966	0.001
Mn^{2+}	2.04	2.035	2.036	0.001
Ni	1.93	1.945	1.94	0.01
Si	1.64	1.655	1.627	0.004
Zn	1.98	1.96	1.960	0.001
Co	1.96	1.96	1.972	0.002
Vac			[2.0]	
Coeff.				
k_1			0.010	0.001
k_2			0.011	0.001
Octahedral bond distances				
Al	1.915	1.91	1.908	0.001
Fe^{2+}	2.16	2.12	2.150	0.002
Fe^{3+}	2.025	2.025	2.025	0.001
Mg	2.10	2.095	2.082	0.002
Mn^{2+}	2.21	2.18	2.191	0.002
Mn^{3+}	2.025	–	2.03	0.01
Cr	1.995	1.995	1.995	0.001
Ni	2.070	2.07	2.06	0.01
Ti	1.985	1.98	1.962	0.001
Si			[1.775]	
Zn	2.120	2.11	2.13	0.01
V	2.020	2.025	2.022	0.007
Co	2.125	2.1	2.11	0.01
Vac	–	–	2.11	0.03

Table 3 Mean values of residuals of crystal-chemical parameters after optimisation of bond distances

	a	*u*	T–O	M–O	m.a.n.$_T$	m.a.n.$_M$	Occ$_T$	Occ$_M$
Mean residual	0.0008	0.0003	0.0038	0.0022	0.14	0.10	0.0003	0.0009
	Al	Fe^{2+}	Fe^{3+}	Mg	Mn^{2+}	Mn^{3+}	Si	
Mean residual	0.004	0.004	0.004	0.005	0.010	0.003	0.004	
	Cr	Zn	V	Ni	Ti	Vac	Co	
Mean residual	0.005	0.003	0.004	0.004	0.003	0.001	0.003	

Mg ferrite with decreasing inversion, whereas previous sets like those used by Hazen and Yang (1999) predict a slight decrease, contrary to experimental evidence.

The accuracy reached in cell parameter prediction also allows the reliability of chemical composition to be checked. For instance, the predicted *a* values for hercynite range from 8.1422 to 8.1466 Å in the inversion range 0.05–0.30 afu, which is reasonably the maximum for this compound. Our predicted values support the hypothesis that the *a* value of 8.1458 Å (Harrison et al. 1998) for synthetic hercynite is closer to stoichiometry than $a = 8.1516$ Å (Larsson et al. 1994). The latter value is ascribable to appreciable amounts of Fe^{3+} substituting for Al, due to insufficient experimental control of oxygen fugacity.

Role of octahedral site on tetrahedral distance

The good agreement obtained between observed and calculated T–O bond lengths using Eq. (8) (Fig. 1b) – which holds for all kinds of cations occupying the tetrahedral site – stresses the role of some octahedral cations on tetrahedral distance. This is consistent with the differing tetrahedral bond distances of the same cation in different spinels like aluminates and ferrites, previously observed by Lucchesi et al. (1998, 1999), and with the results of O'Neill (1992) and Waerenborgh et al. (1994). Instead, no influence of tetrahedral cations on M–O distance was detected. This is not surprising, since the T site has $\bar{4}3m$ symmetry, with six equivalent unshared edges and no angular freedom, and consequently different cations in the T site can only modify the T–O distance. The M site has $\bar{3}m$ symmetry, with six unshared edges, pertaining to the faces perpendicular to the threefold axis, and six shared edges; the octahedral angle O–M–O (O–O is a shared edge) is 90° only for $u = 1/4$. Cations entering the M site can modify not only the M–O distance but also the octahedral angle. Given M–O and O–M–O, all the other geometric parameters can be determined, including T–O distance (see Appendix 1). This distance, of course, is mainly determined by cation size, but it may also be appreciably modified by some octahedral cations via a decrease in the O–M–O angle.

Applications

Some literature problems concerning cation distribution and data consistency are now examined. Results were obtained using the SIDR program (available from the authors). All reported cation fractions are rounded to the third decimal point since, as we will see, the uncertainty is definitely greater than 0.001 afu.

Table 4 Observed and calculated crystal chemical parameters of a natural spinel (Della Giusta et al. 1986) and optimised cation distribution. See Fig. 2 for uncertainties

	O_j	σ_j	C_j	C_j–O_j
$F(X_i) = 0.07$				
a	8.1230	0.0005	8.1230	0.0000
u	0.2623	0.0002	0.2624	0.0001
T–O	1.9317	0.0028	1.9327	0.0010
M–O	1.9360	0.0015	1.9355	−0.0005
m.a.n.$_T$	15.22	0.24	15.19	−0.03
m.a.n.$_M$	13.99	0.39	13.94	−0.05
Mg	0.787	0.002	0.786	0.001
Fe^{2+}	0.215	0.003	0.214	0.001
Al	1.815	0.007	1.818	0.003
Cr	0.146	0.001	0.146	0
	Cation distribution			
	T		M	
Al	0.206		1.612	
Fe^{2+}	0.207		0.007	
Mg	0.579		0.207	

Cation distribution of a natural spinel

A natural spinel with composition $Mg_{0.787}Fe^{2+}_{0.215}Al_{1.815}Cr_{0.146}O_4$ (LE20, Della Giusta et al. 1986) with three cations (Mg, Al, Fe^{2+}) entering both sites is considered. Minimisation results are listed in Table 4. There is very good agreement between observed and calculated parameters, supported by the low $F(X_i)$ value.

Since the values of the atomic fractions are strongly correlated by crystal chemical constraints, evaluation of their standard deviations is not easy. Nevertheless, the reliability of the resulting distribution can be tested by scanning $F(X_i)$ at fixed values of each atomic fraction X_i in a range around the minimum. For good-quality data, with cations sufficiently different in atomic number and/or bond distances, as in this example, $F(X_i)$ shows parabolic behaviour (Fig. 2). The parabola for Mg and Al is wider than that of Fe^{2+} because the latter is restrained by both m.a.n. and bond distances. Mg and Al contents are essentially restrained by bond distances, as their atomic numbers are similar. The variation of each atomic fraction which leads to doubling of the minimised $F(X_i)$ may be assumed as the uncertainty of its

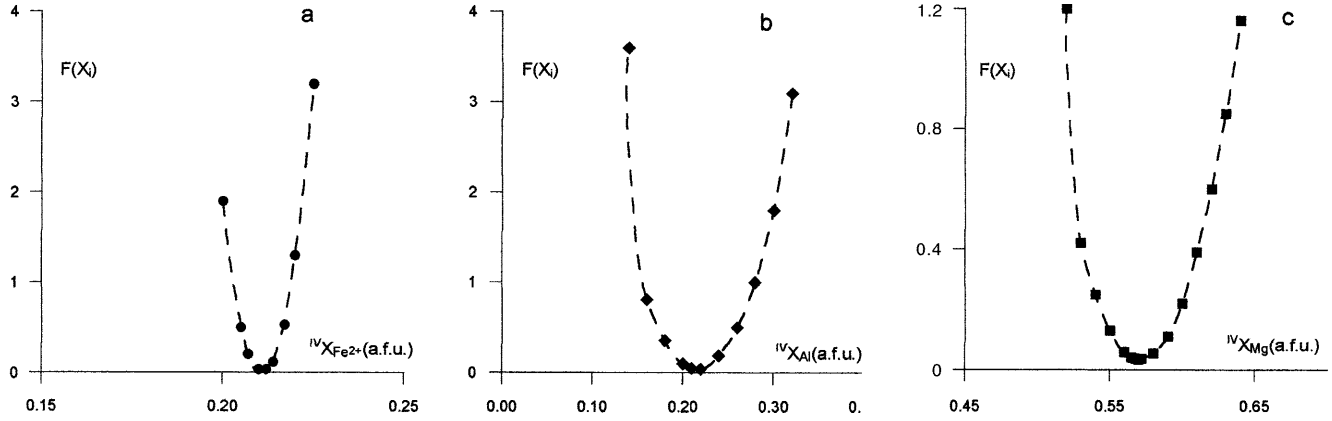

Fig. 2 Parabolic trend of $F(X_i)$ according to tetrahedral atomic fractions. Variations of X_i causing doubling of $F(X_i)$ may be assumed as uncertainty

optimised value. In this case, estimated uncertainties for ${}^{IV}X_{Fe^{2+}}$, ${}^{IV}X_{Al}$ and ${}^{IV}X_{Mg}$ are 0.004, 0.015 and 0.018 afu, respectively.

Distribution in a defect spinel

Foley et al. (2001), in a study of optimisation of site occupancies, examined a synthetic spinel of composition $(Mg_{0.70}Fe_{0.23})Al_{1.97}O_4$, previously investigated in Pavese et al. (1999), using neutron scattering and Mössbauer spectroscopy. These authors propose rather different cation distributions at ambient temperature (Table 5A, B), but both give high residuals of bond distances.

Foley et al. (2001) in their Fig. 1 report very small bond length residuals in the T site, but still as large as 0.01 Å in the M site. This leads to an unacceptable discrepancies between calculated and observed cell parameter (close to 0.02 Å). As previously stated, we regard such a discrepancy as a threshold to exclude unreliable samples from the database.

Cation distribution C was obtained by assigning to T and M sites m.a.n. values of 14.07 and 12.95, consistent with both distributions A and B, with relatively large standard deviations, 0.5 and 0.3 respectively. The tetrahedral vacancy distance was provisionally assigned to 2.00 Å, since the value of 2.078 Å assigned by Chassagneux et al. (1985) seems too high on the basis of experimental evidence (work in progress). In any case, due to its relative scarcity, its value is of secondary importance in this example.

Distribution C requires a definitely higher Mg–Al disorder, ${}^{IV}X_{Al} = 0.35$ afu, which is consistent both with the very high temperature (1600 °C) of the powder synthesis, and the amounts of ${}^{IV}X_{Al}$ (0.40–0.47 afu) determined by Lucchesi and Della Giusta (1994), in a defect, iron-free MgAl spinel whose vacancy content was similar. It is emphasised that the ${}^{IV}X_{Fe^{3+}}$ obtained from minimisation is fully consistent with Mössbauer results, and that minimisation leads to Fe^{3+} ordering in the T site, in spite of the initial random distribution between T and M. Figure 3 shows the changes in $F(X_i)$ with the T-site atomic fractions of Al and vacancy. The Al fraction is heavily dependent on the $F(X_i)$ value, which increases rapidly for small changes in ${}^{IV}X_{Al}$. Its uncertainty can be estimated as being close to 0.01 afu, as in the present example. Vacancies seem to be preferentially ordered in the T site, but the influence on the value of the function is definitely weaker.

Table 5 Comparison of cation distributions obtained for a synthetic spinel by **A** Pavese et al. 1999; **B** Wright et al. 2000; **C** present paper

	Observed parameters	Calculated parameters		
		A	**B**	**C**
a	8.067(2)	8.0714	8.0713	8.0670
u	0.2598(1)	0.2632	0.2614	0.2598
T–O	1.8835(14)	1.9300	1.9069	1.8834
M–O	1.9409(7)	1.9183	1.9302	1.9410
Mg	0.70	0.700	0.706	0.703
Al	1.97	1.971	1.964	1.966
Fe^{3+}	0.23	0.230	0.231	0.232
Vacancy	0.10	0.100	0.099	0.101
Sum	3.00	3.001	3.000	3.002
Valence	8.00	8.002	7.998	8.000
$F(X_i)$		262	68	0.099
		Cation distribution		
T site				
Mg		0.588	0.463	0.392
Al		0.082	0.226	0.349
Fe^{3+}		0.230	0.212	0.195
Vacancy		0.100	0.099	0.064
Sum		1.000	1.000	1.000
M site				
Mg		0.056	0.121	0.154
Al		0.944	0.869	0.811
Fe^{3+}		0.000	0.009	0.017
Vacancy		0.000	0.000	0.018
Sum		1.000	1.000	1.000

Cation distribution in $(Fe,Mn)_2TiO_4$

Sedler et al. (1994) used the Rietveld method to study this solid solution, which also contains appreciable

amounts of trivalent iron, synthesised at 950 °C. They did not use site occupancies as variable parameters, but changed the cation distribution stepwise. They proposed, all along the join, an almost constant inversion of about 0.90, corresponding to about 0.10 afu of Ti in T site. No conclusions were drawn about Fe^{2+}, Fe^{3+} or Mn^{2+} distributions. This is a complex situation, since these three cations can only be distributed on the basis of their site bond distances, due to the similar atomic numbers of Fe and Mn. Since Sedler et al. (1994) do not report T and M site m.a.n., we recalculated these parameters from the proposed inversion, assigning them standard deviations consistent with other Rietveld refinements. Table 6 reports the cation distribution obtained with SIDR for sample D–08 of Sedler et al. (1994): all the structural and chemical parameters are satisfactorily reproduced and $F(X_i)$ reaches a very low value, 0.079. This value is obtained with full ordering of Ti^{4+} in M site and preferential ordering of Mn^{2+} in T site.

Figure 4 shows that $F(X_i)$ has poorly defined minimum values with respect to the changes in Fe and Mn atomic fractions, and a rather irregular trend, due to the high number of exchanging cations (four) with similar scattering power. In any case, in Fig. 4 the preference of Ti for M site is clear, and the suggested distribution for Fe and Mn is consistent with their usual behaviour in spinel structure. Similar results are obtained all along the join.

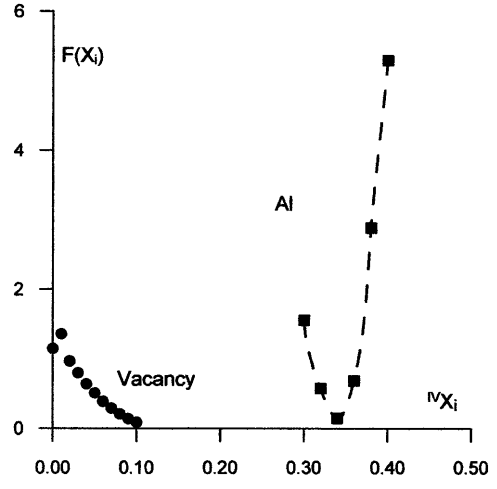

Fig. 3 Trend of $F(X_i)$ as a function of Al and vacancies in T site

Table 6 Cation distribution obtained for $(Fe,Mn)_2TiO_4$ (Sedler et al. 1994)

	O_j	σ_j	C_j	C_j–O_j
$F(X_i)$ = 0.08				
a	8.6017	0.0001	8.6017	0.0000
u	0.2606	0.0002	0.2605	0.0001
T–O	2.020	0.003	2.020	0.000
M–O	2.063	0.002	2.064	0.001
$m.a.n._T$	25.6		25.4	
$m.a.n._M$	24.1		24.0	
Fe^{2+}	0.965		0.964	−0.002
Fe^{3+}	0.088		0.087	−0.001
Mn^{2+}	0.991		0.991	−0.001
Ti	0.956		0.957	0.000
Sum	3.000		2.999	
	Cation distribution			
	T		M	
Fe^{2+}	0.310		0.326	
Fe^{3+}	0.045		0.021	
Mn^{2+}	0.644		0.174	
Ti	0.000		0.479	
Sum	0.999		1.000	

Conclusions

– Using a database containing 295 samples, a new set of cation-to-oxygen bond distances was optimised for spinel structure, allowing more accurate predictions about its behaviour.

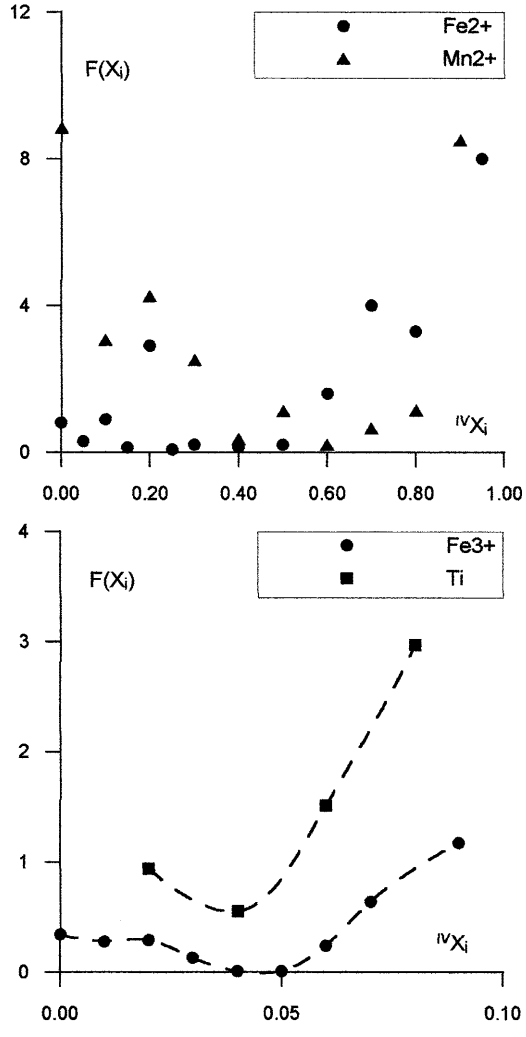

Fig. 4 Trend of $F(X_i)$ as a function of tetrahedral cations. Due to similarity of atomic number, trend is rather irregular and minimum is poorly defined except for Ti and, subordinately, Fe^{3+}. Strong ordering of Mn in T site is in any case indicated

- The influence of octahedral cations on tetrahedral bond distance was clearly evidenced, and is related to modifications in the octahedron angle in the presence of Fe^{3+} and Ni^{2+}.
- The improved procedure is very helpful in determining cation distributions accurately. It also allows the reliability of the chemical composition and inconsistencies in experimental data to be checked.
- Determination of standard deviations of all experimental data is crucial, since the distributions obtained with our procedure are quite sensitive to this parameter. It should be recalled that different refinement strategies applied to spinel structure can lead to very small standard deviations but also to atomic fractions differing by much more than 3σ of any single determination. Unfortunately, this point has seldom been discussed, even in recent papers.
- The number of cations exchanging between T and M whose site atomic fractions can be determined depends not only on the quality of the experimental data but also on differences among atomic numbers and bond distances. Whenever these parameters differ, distributions involving up to three to four cations per site can be determined with satisfactory reliability.
- Within the accuracy of the database, we can assume, as a mean, approximately 0.01 afu as a realistic uncertainty value for major atomic fractions.

Acknowledgements Thanks are due to the reviewers for comments and suggestion. Ms. Gabriel Walton revised the English text. This work benefited from the financial support of MURST (Transformations, reactions, ordering in minerals).

Appendix 1

The general formula of oxide spinels is AB_2O_4, and the distribution configuration is represented as $^{IV}(A_{1-x}B_x)\,^{VI}(B_{2-x}A_x)O_4$. *Normal* spinels have $x = 0$, whereas *inverse* spinels have $x = 1$; any distribution is possible between the extremes.

The unit cell of spinel is cubic, space group $Fd\bar{3}m$, with a cell edge close to 8 Å. It contains 32 equivalent oxygen anions in a site with point symmetry $\bar{3}m$, having coordinates (u,u,u), u ranging from 0.24 to 0.27 (space group no. 227, origin at centre $\bar{3}m$). Cations are arranged in a tetrahedral T site and an octahedral M site. T site has point symmetry $\bar{4}3m$, multiplicity 8 and coordinates 0,0,0; M site has point symmetry $\bar{3}m$, multiplicity 16 and coordinates 1/2, 1/2, 1/2. A full description of spinel structure geometry includes cell edge, u, T–O and M–O bond distances, a tetrahedral unshared edge, an octahedral unshared edge, an octahedral edge shared with other octahedra, and an octahedral O–M–O angle. Given any two of these, all the others can be easily be calculated (Hill et al. 1979) using the following equations:

$$a = \frac{8}{11\sqrt{3}}\left[5\mathrm{TO} + \sqrt{33(\mathrm{MO})^2 - 8(\mathrm{TO})^2}\right] \tag{A1}$$

$$u = \frac{0.75\dfrac{\mathrm{MO}^2}{\mathrm{TO}^2} - 2 + \sqrt{\dfrac{33}{16}\dfrac{\mathrm{MO}^2}{\mathrm{TO}^2} - 0.5}}{6\left(\dfrac{\mathrm{MO}^2}{\mathrm{TO}^2} - 1\right)} \tag{A2}$$

$$\mathrm{MO} = a\sqrt{\left(\frac{1}{2} - u\right)^2 + 2\left(\frac{1}{4} - u\right)^2} \tag{A3}$$

$$\mathrm{T{-}O} = a\sqrt{3\left(\frac{1}{8} - u\right)^2} \tag{A4}$$

$$\mathrm{T{-}T} = a\frac{\sqrt{3}}{4} \tag{A5}$$

$$\mathrm{M{-}M} = a\frac{\sqrt{2}}{4} \tag{A6}$$

$$\mathrm{T{-}M} = a\frac{\sqrt{11}}{8} \tag{A7}$$

$$^{\mathrm{IV}}\mathrm{O{-}O} = a\sqrt{2(2u - 0.25)^2} \tag{A8}$$

$$^{\mathrm{VI}}\mathrm{O{-}O_{sh}} = a\sqrt{2(0.75 - 2u)^2} \tag{A9}$$

$$^{\mathrm{VI}}\mathrm{O{-}O_{unsh}} = a\sqrt{4u^2 - 2u + 0.375} \tag{A10}$$

$$\mathrm{OMO(rad)} = \arccos\left[\frac{1 - 2(0.75 - 2u)^2}{2(3u^2 - 2u + 0.375)}\right] \tag{A11}$$

OMO is the octahedral angle and O–O the shared edge.

References

Andreozzi GB, Princivalle F, Skogby H, Della Giusta A (2000) Cation ordering and structural variations with temperature in $MgAl_2O_4$ spinel: an X-ray single-crystal study. Am Mineral 85: 1164–1171

Brese NE, O'Keeffe M (1991) Bond-valence parameters for solids. Acta Crystallogr (B) 47: 192–197

Brown ID, Altermatt D (1985) Bond-valence parameters obtained from a systematic analysis of the inorganic crystal structure database. Acta Crystallogr (B) 41: 244–247

Chassagneux F, Rousset A, Redoules JP (1985) Elaboration et caractérisation de chromites de fer(III) a structure spinelle lacunaire. J Solid State Chem 56: 74–83

Della Giusta A, Ottonello G (1993) Energy and long-range disorder in simple spinels. Phys Chem Miner 20: 228–241

Della Giusta A, Princivalle F, Carbonin S (1986) Crystal chemistry of a suite of natural Cr-bearing spinels with $0.15 \le Cr \le 1.07$. N Jb Miner Abh 155: 319–330

Della Giusta A, Carbonin S, Ottonello G (1996) Temperature-dependent disorder in a natural Mg–Al–Fe^{2+}–Fe^{3+} spinel. Mineral Mag 60: 603–616

Fleet ME (1981) The structure of magnetite. Acta Crystallogr (B) 37: 917–920

Foley JA, Wright SE, Hughes JM (2001) Cation partitioning versus temperature in spinel: optimization of site occupants. Phys Chem Miner 28: 143–149

Hafner S (1960) Metalloxyde mit Spinellstruktur. Schweiz Mineral Petrogr Mitt 40: 207–242

Hamilton WC (1958) Neutron diffraction investigation of the 119 K transition in magnetite. Phys Rev 110: 3–5

Harrison RJ, Redfern SAT, O'Neill HStC (1998) The temperature dependence of the cation distribution in synthetic hercynite ($FeAl_2O_4$) from in-situ neutron structure refinements. Am Mineral 83: 1092–1099

Hawthorne FC, Ungaretti L, Oberti R (1995) Site populations in minerals: terminology and presentation of results of crystal-structure refinement. Can Mineral 33: 907–911

Hazen RM, Yang H (1999) Effects of cation substitution and order-disorder on P–V–T equations of state of cubic spinels. Am Mineral 84: 1956–1960

Hill RJ, Craig JR, Gibbs GV (1979) Systematics of the spinel structure type. Phys Chem Miner 4: 317–339

James F, Roos M (1975) Minuit-A system for function minimization and analysis of the parameter errors and correlations. Comp Phys Comm 10: 343–367

Larsson L, O'Neill HStC, Annersten H (1994) Crystal chemistry of the synthetic hercynite ($FeAl_2O_4$) form XRD structural refinements and Mössbauer spectroscopy. Eur J Mineral 6: 39–51

Lucchesi S, Della Giusta A (1994) Crystal chemistry of non-stoichiometric Mg–Al synthetic spinels. Z Kristallogr 209: 714–719

Lucchesi S, Della Giusta A, Russo U (1998) Cation distribution in natural Zn-aluminate spinels. Mineral Mag 62: 41–54

Lucchesi S, Russo U, Della Giusta A (1999) Cation distribution in natural Zn-spinels: franklinite. Eur J Mineral 11: 501–511

Maekawa H, Kato S, Kawamura K, Yokokawa T (1997) Cation mixing in natural $MgAl_2O_4$ spinel: a high-temperature ^{27}Al NMR study. Am Mineral 82: 1125–1132

Marshall CP, Dollase WA (1984) Cation arrangement in iron-zinc-chromium spinel oxides. Am Mineral 69: 928–936

O'Neill HStC (1992) Temperature dependence of the cation distribution in zinc ferrite ($ZnFe_2O_4$) from powder XRD structural refinements. Eur J Mineral 4: 571–580

O'Neill HStC, Navrotsky A (1983) Simple spinels: crystallographic parameters, cation radii, lattice energies and cation distributions. Am Mineral 68: 181–194

O'Neill HStC, Navrotsky A (1984) Cation distributions and thermodynamic properties of binary spinel solid solutions. Am Mineral 69: 733–753

O'Neill HStC, Annersten H, Virgo D (1992) The temperature dependence of the cation distribution in magnesioferrite ($MgFe_2O_4$) from powder XRD structural refinements and Mössbauer spectroscopy. Am Mineral 77: 725–740

Pavese A, Artioli G, Russo U, Hoser A (1999) Cation partitioning versus temperature in $(Mg_{0.70}Fe_{0.23})Al_{1.97}O_4$ synthetic spinel by in situ neutron powder diffraction. Phys Chem Miner 26: 242–250

Ross NL, Shu JF, Hazen RM, Gasparik T (1990) High-pressure crystal chemistry of stishovite. Am Mineral 75: 739–747

Sedler IK, Feenstra A, Peters T (1994) An X-ray powder diffraction study of synthetic $(Fe,Mn)_2TiO_4$ spinel. Eur J Mineral 6: 873–885

Shannon RD (1976) Revised effective ionic radii and systematic studies of interatomic distances in halides and chalcogenides. Acta Crystallogr (A) 32: 751–767

Waerenborgh JC, Figueiredo MO, Cabral JMP, Pereira LCJ (1994) Temperature and composition dependence of the cation distribution in synthetic $ZnFe_yAl_{2-y}O_4$ ($0 \le y \le 1$) spinels. J Solid State Chem 111: 300–309

Wechsler BA, Lindsley DH, Prewitt CT (1984) Crystal structure and cation distribution in titanomagnetites ($Fe_{3-x}Ti_xO_4$). Am Mineral 69: 754–770

Wright SE, Foley JA, Hughes JM (2000) Optimization of site occupancies in minerals using quadratic programming. Am Mineral 85: 524–531